

# NV-center microscopy a versatile tool to study magnetism

Aurore Finco

Laboratoire Charles Coulomb  
Team Solid-State Quantum Technologies (S2QT)

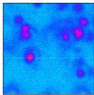
CNRS and Université de Montpellier, Montpellier, France



ITN-SPEAR, FTS5: Skyrmions, February 28<sup>th</sup> 2024, Hamburg

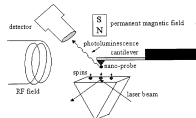
slides available at <https://magimag.eu>

# A very short history



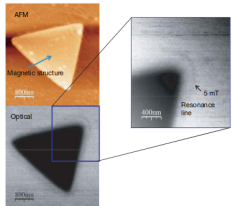
**1997:** First detection of single NV centers

■ A. Gruber *et al.* *Science* 276 (1997), 2012



**2004:** Proposal of the scanning NV center magnetometer

■ B. M. Chernobrod and G. P. Berman. *J. Appl. Phys.* 97 (2004), 014903

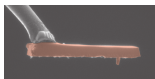


**2008:** First demonstration of scanning NV imaging

■ G. Balasubramanian *et al.* *Nature* 455 (2008), 648–651

**2012:** All-diamond probes

■ P. Maletinsky *et al.* *Nat. Nano.* 7 (2012), 320–324



**2020:** Commercial scanning NV microscopes available

# Further reading

Reviews about NV center magnetometry:

- S. Hong *et al.* *MRS Bulletin* 38 (2013), 155–161
- L. Rondin *et al.* *Reports on Progress in Physics* 77 (2014), 056503
- F. Casola *et al.* *Nature Reviews Materials* 3 (2018), 17088
- A. Laraoui and K. Ambal. *Applied Physics Letters* 121 (2022), 060502
- Y. Xu *et al.* *Photonics Research* 11 (2023), 393–412
- A. Finco and V. Jacques. *APL Materials* 11 (2023), 100901

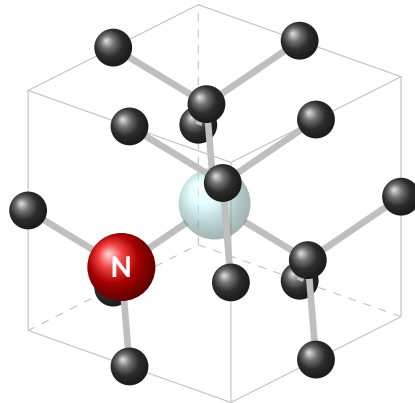
# Outline

1. The NV center in diamond as a quantum sensor
2. Dismantling the scanning NV microscope
3. Quantitative ODMR experiments
  - Principle of the measurement
  - The need for a proper calibration
  - Example 1: analyzing domain walls
  - Example 2: the spin cycloid in bismuth ferrite
  - Example 3: van der Waals magnets
4. Taking a step back: PL quenching effects
  - Strong off-axis magnetic fields
  - Magnetic noise!
5. Relaxometry: sensing via the relaxation time
6. Coherent control of the NV center using spin waves
7. Going further: other sensors and sensing methods

# Outline

1. The NV center in diamond as a quantum sensor
2. Dismantling the scanning NV microscope
3. Quantitative ODMR experiments
  - Principle of the measurement
  - The need for a proper calibration
  - Example 1: analyzing domain walls
  - Example 2: the spin cycloid in bismuth ferrite
  - Example 3: van der Waals magnets
4. Taking a step back: PL quenching effects
  - Strong off-axis magnetic fields
  - Magnetic noise!
5. Relaxometry: sensing via the relaxation time
6. Coherent control of the NV center using spin waves
7. Going further: other sensors and sensing methods

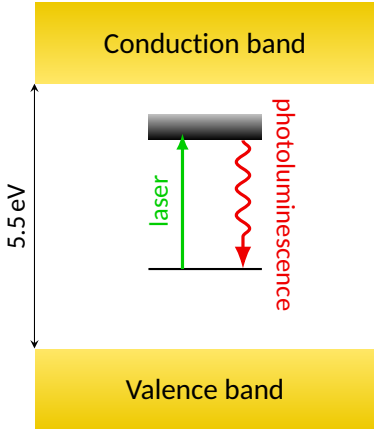
# The NV center in diamond



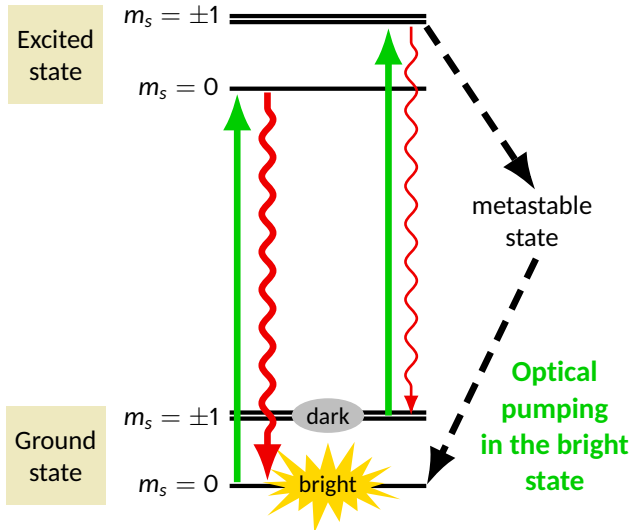
- Artificial atom: energy levels in the diamond bandgap
- Photostable defect
- Spin  $S=1$
- Individual defects can be isolated/implanted
- Ambient conditions

# Optical properties

Artificial atom  
in the diamond band gap

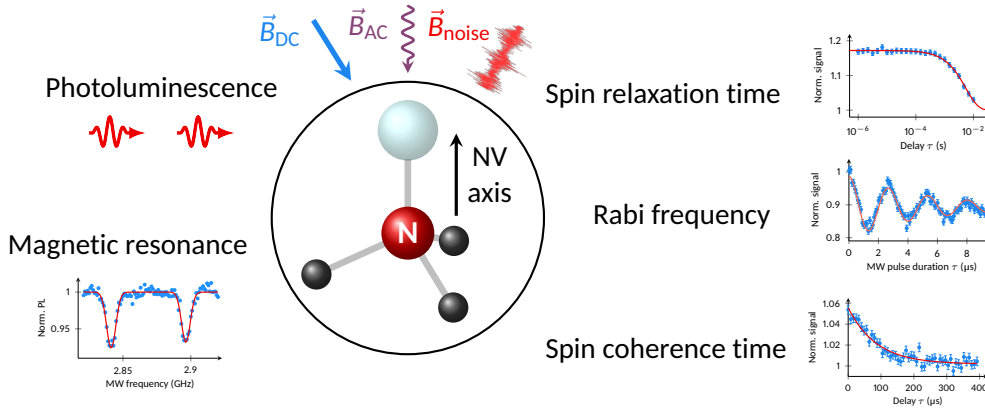


Spin dependent photoluminescence



# The NV center as a quantum sensor

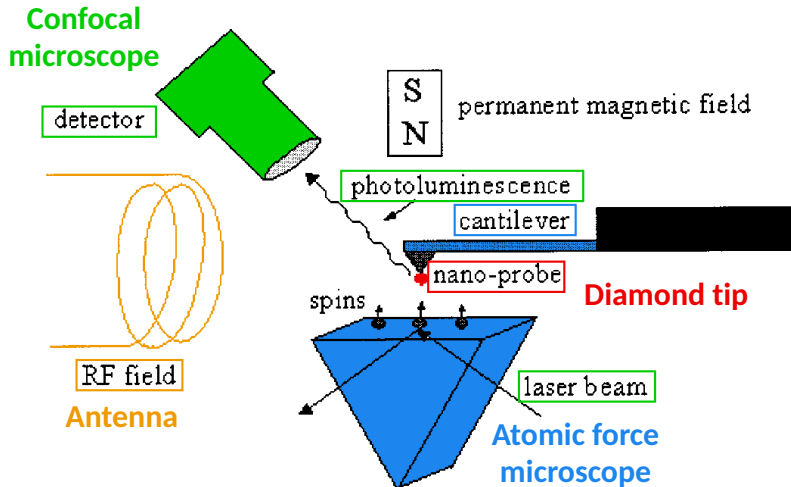
$$\mathcal{H}_{\text{gs}} = \hbar \left[ D_{\text{NV}} \hat{S}_z^2 + \gamma_{\text{NV}} \hat{\vec{S}} \cdot \vec{B} \right] \text{ with } \begin{cases} D_{\text{NV}} \simeq 2.87 \text{ GHz} \\ \gamma_{\text{NV}} \simeq 28 \text{ GHz T}^{-1} \end{cases}$$



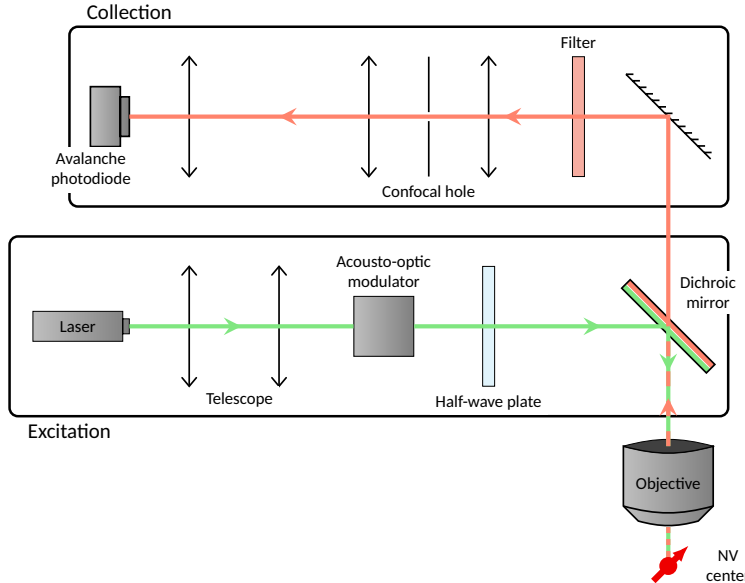
# Outline

1. The NV center in diamond as a quantum sensor
2. **Dismantling the scanning NV microscope**
3. Quantitative ODMR experiments
  - Principle of the measurement
  - The need for a proper calibration
  - Example 1: analyzing domain walls
  - Example 2: the spin cycloid in bismuth ferrite
  - Example 3: van der Waals magnets
4. Taking a step back: PL quenching effects
  - Strong off-axis magnetic fields
  - Magnetic noise!
5. Relaxometry: sensing via the relaxation time
6. Coherent control of the NV center using spin waves
7. Going further: other sensors and sensing methods

# Dismantling the scanning NV microscope



# The confocal microscope



# The atomic force microscope

Akiyama probes

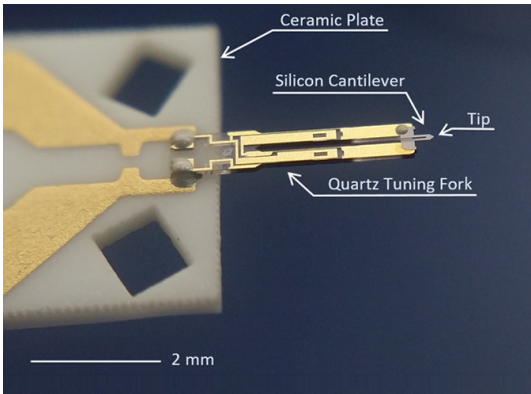


Image from [www.akiyamaprobe.com](http://www.akiyamaprobe.com)

- The quartz tuning fork oscillates at about 32 kHz.
- The tip and cantilever are removed and the diamond tip glued on one of the arms.
- Excitation and reading of the mechanical resonance with piezo elements.
- Feedback loop onto the frequency or the amplitude of the mechanical resonance.

# The diamond probes

All-diamond probes developed in 2012

■ P. Maletinsky *et al.* *Nat. Nano.* 7 (2012), 320–324

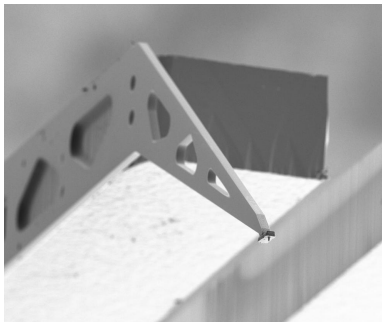


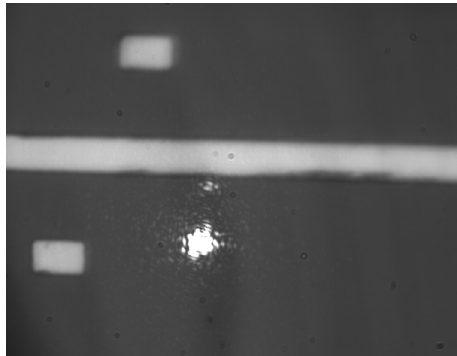
Image from [www.qzabre.com](http://www.qzabre.com)

- High-purity diamond  
→ Good coherence properties
- Hosting single NV centers at 50-100 nm from the sample surface  
→ Spatial resolution of the microscope
- Usually made from (001) diamond  
→ Tilted NV axis
- Diamond pillar as guide for the emitted light  
→ Optimized signal collection

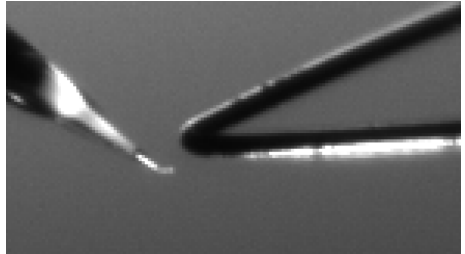
# The microwave antenna

We need to deliver a microwave signal very close to the NV center. Several options:

Patterned gold line on the sample



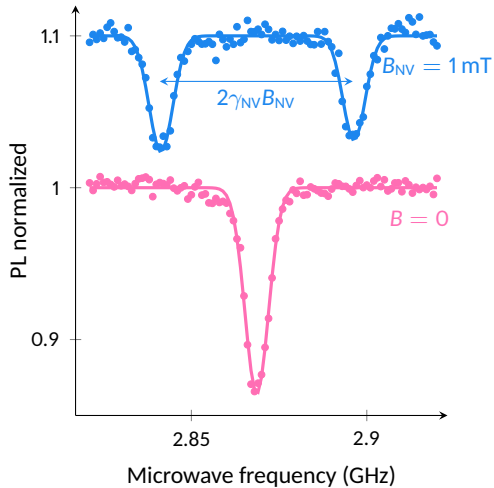
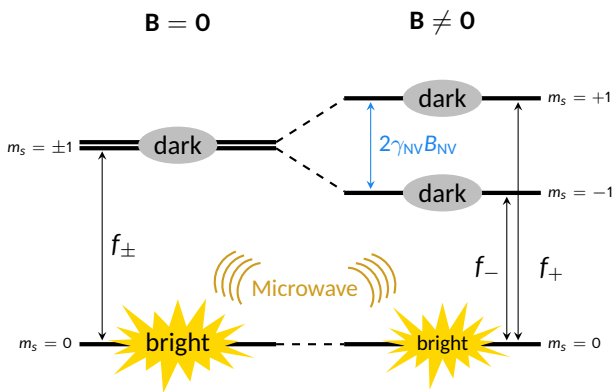
Use a wire, close to the tip



# Outline

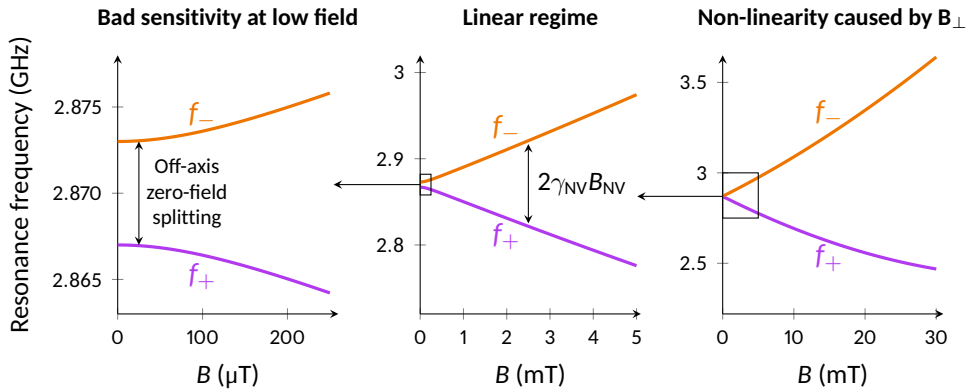
1. The NV center in diamond as a quantum sensor
2. Dismantling the scanning NV microscope
3. Quantitative ODMR experiments
  - Principle of the measurement
  - The need for a proper calibration
  - Example 1: analyzing domain walls
  - Example 2: the spin cycloid in bismuth ferrite
  - Example 3: van der Waals magnets
4. Taking a step back: PL quenching effects
  - Strong off-axis magnetic fields
  - Magnetic noise!
5. Relaxometry: sensing via the relaxation time
6. Coherent control of the NV center using spin waves
7. Going further: other sensors and sensing methods

# Optically detected magnetic resonance (ODMR)



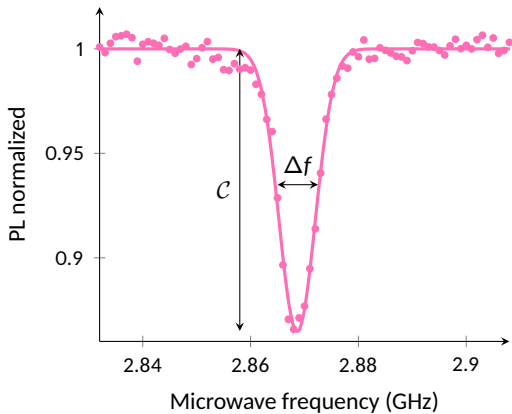
# The different regimes

Calculation of  $f_-$  and  $f_+$ , with a  $45^\circ$  angle between  $\vec{B}$  and the NV axis



- We apply a bias field roughly aligned with the NV axis (also to extract the sign of  $B_{\text{NV}}$ )
- Quantitative measurements of very strong fields impossible

# Magnetic field sensitivity



$$\eta_B = \frac{4}{3\sqrt{3} \gamma_{\text{NV}}} \frac{\Delta f}{\mathcal{C} \sqrt{\mathcal{R}}}$$

- Linewidth  $\Delta f$ : tunable with the **microwave** power
  - Contrast  $\mathcal{C}$ : tunable with the **laser** and the **microwave** power
  - Off-resonance count rate  $\mathcal{R}$ : tunable with the **laser** power
- Optimal ( $P_{\text{laser}}$ ,  $P_{\text{MW}}$ ) values  
→ Sensitivity: a few  $\mu\text{T}/\sqrt{\text{Hz}}$

# Understanding stray field maps

$$\vec{B} = \mu_0 \vec{\nabla} \phi$$

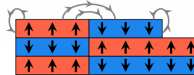
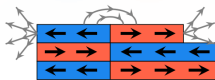
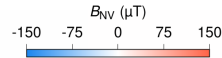
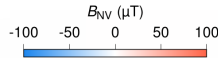
where  $\phi$  is a scalar potential which verifies the Poisson equation:

$$\Delta \phi = \vec{\nabla} \cdot \vec{M}$$

Same equation as for the electrostatic potential  $V$

$$\Delta V = -\frac{\rho}{\epsilon_0}$$

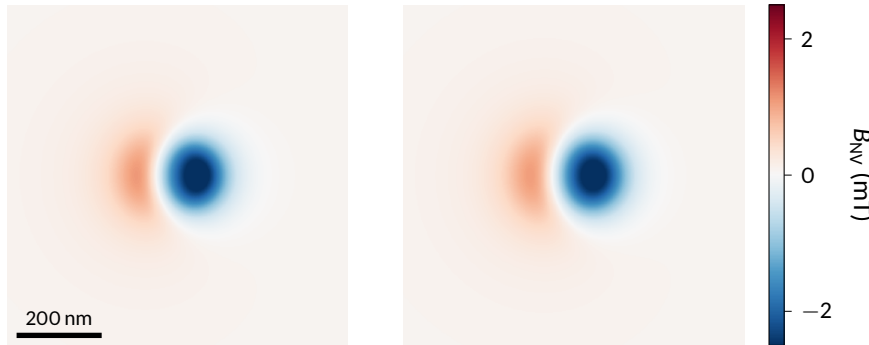
$\Rightarrow \vec{\nabla} \cdot \vec{M}$  can be seen as the magnetic field source



Field sources: edges, domain walls, skyrmions, etc.

# We need to calibrate the NV flying distance!

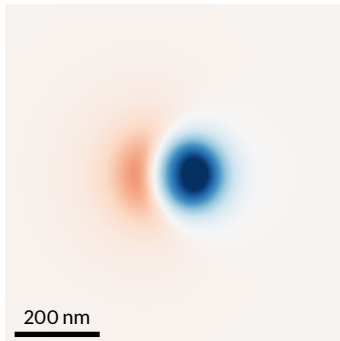
Simulated stray field maps from skyrmions of diameter 150 nm in a 0.5 nm thick film with  $M_s = 1 \text{ MA m}^{-1}$



# We need to calibrate the NV flying distance!

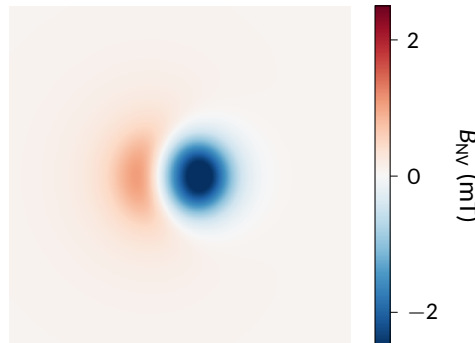
Simulated stray field maps from skyrmions of diameter 150 nm in a 0.5 nm thick film with  $M_s = 1 \text{ MA m}^{-1}$

Clockwise Néel skyrmion



NV height:  $d_{\text{NV}} = 50 \text{ nm}$   
DW width:  $w = 15 \text{ nm}$

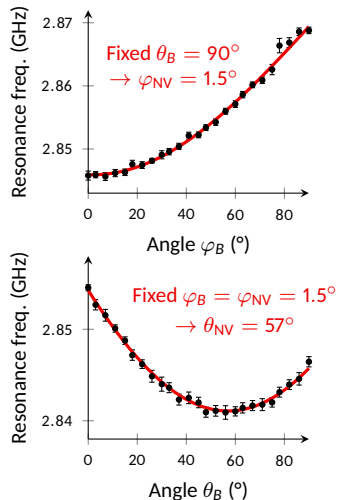
Counter clockwise Néel skyrmion



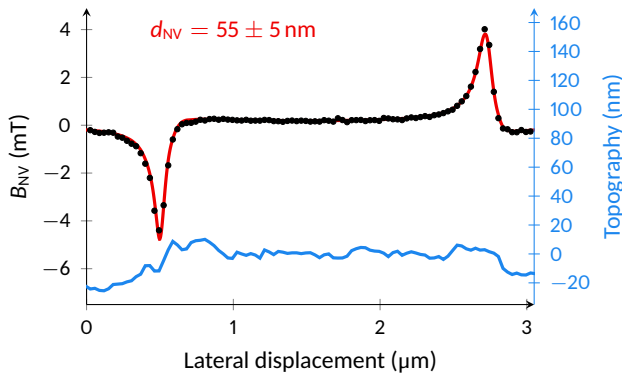
NV height:  $d_{\text{NV}} = 80 \text{ nm}$   
DW width:  $w = 30 \text{ nm}$

# The calibration procedure

## 1. Find the NV axis orientation



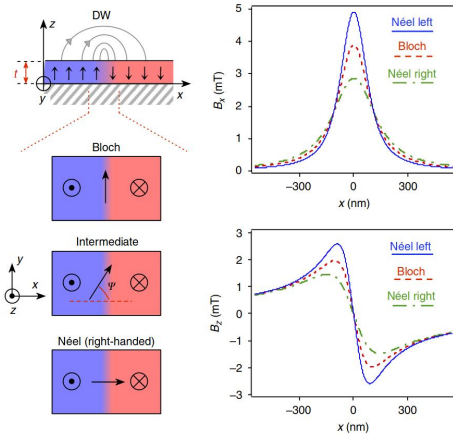
## 2. Find the NV height $d_{NV}$ with a well-known ferromagnetic stripe



T. Hingant et al. Phys. Rev. Appl. 4 (2015), 014003

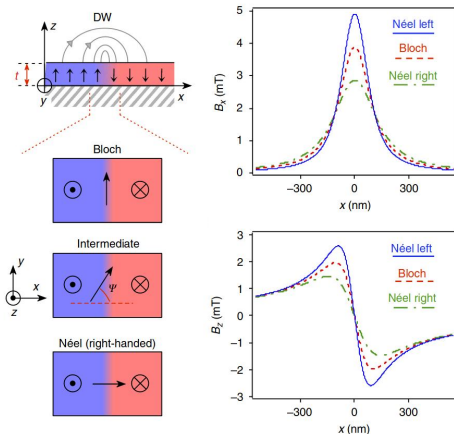
# Example 1: analysis of domain walls

Analytical expression of the stray field

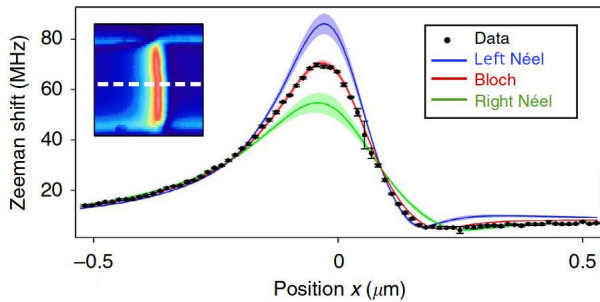


# Example 1: analysis of domain walls

Analytical expression of the stray field



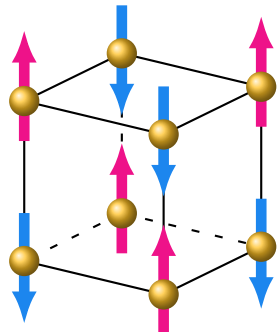
Ta/CoFeB/MgO stripe



→ With a precise calibration, we can determine the internal texture of the domain wall

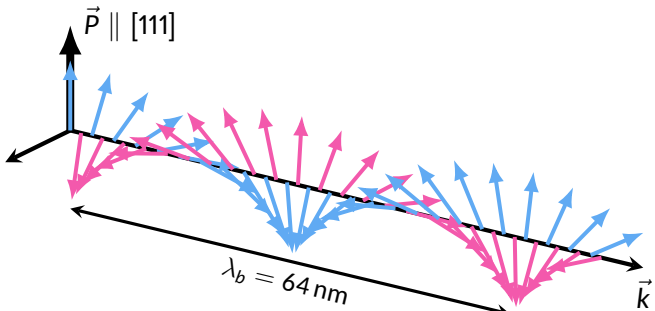
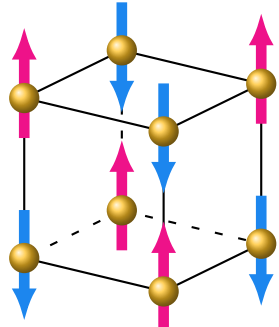
## Example 2: the cycloid in bismuth ferrite

G-type antiferromagnet



# Example 2: the cycloid in bismuth ferrite

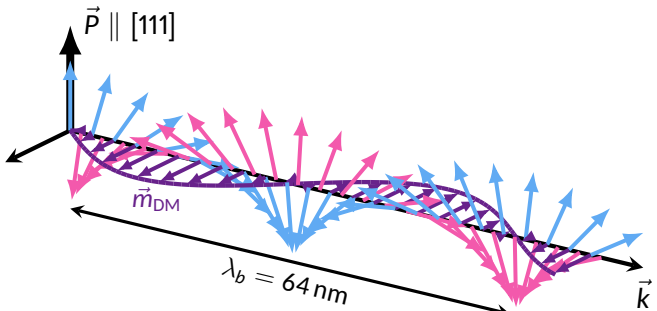
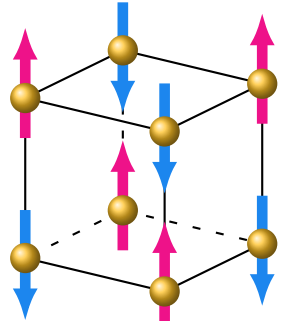
G-type antiferromagnet



Fully compensated cycloid  
→ **No stray field!**

# Example 2: the cycloid in bismuth ferrite

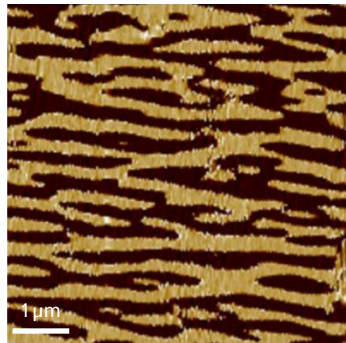
G-type antiferromagnet



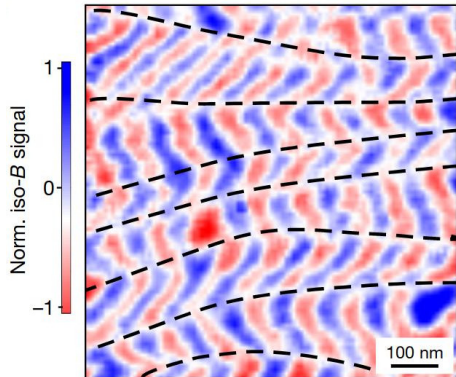
Spin density wave  
Weak uncompensated moment  
→ **Small stray field**

# First real-space images of the cycloid

Piezoresponse force microscopy image  
Ferroelectric domains



NV image  
Field from the spin density wave

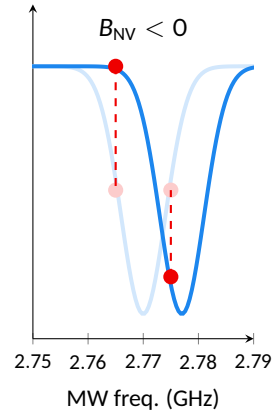
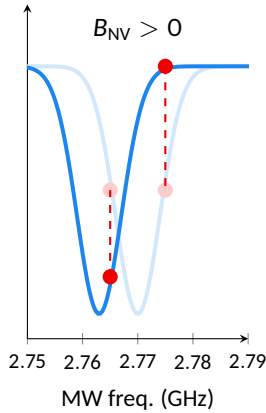
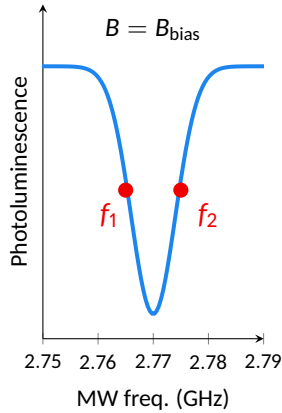


**Reminder:** The wavevector  $\vec{k}$  of the cycloid  
is always **perpendicular** to  $\vec{P}$

I. Gross et al. *Nature* 549 (2017), 252–256

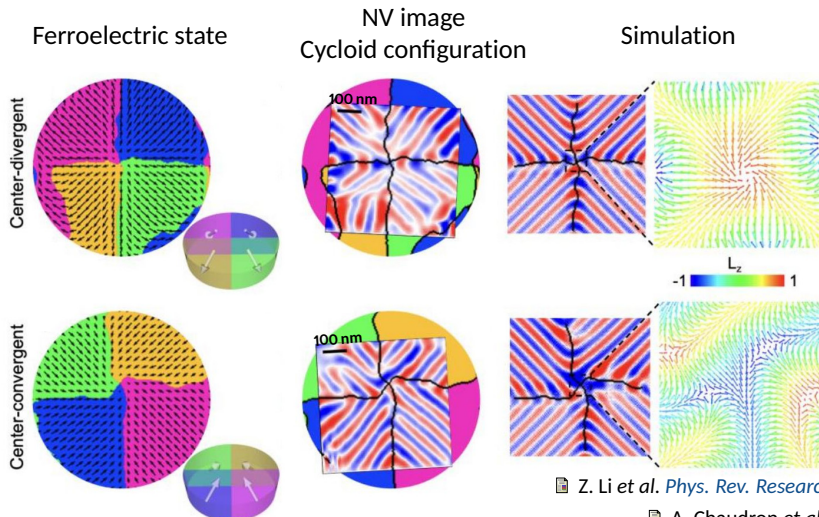
# Note: the iso-B mode

$$\Delta PL = PL(f_2) - PL(f_1)$$



# Creating "topological" multiferroic states in BiFeO<sub>3</sub>

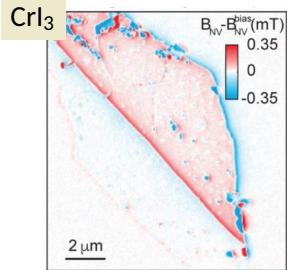
Collaboration: Lab. A. Fert, Paris (A. Chaudron, K. Bouzehouane, S. Fusil, V. Garcia)



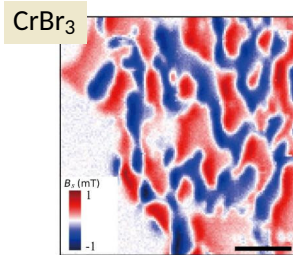
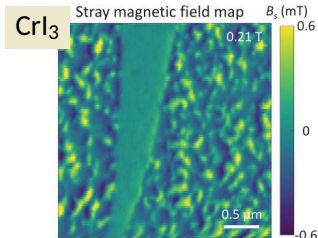
■ Z. Li et al. *Phys. Rev. Research* 5 (2023), 043109

■ A. Chaudron et al. *submitted* (2024)

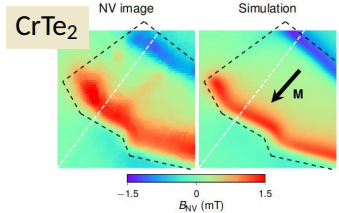
# Example 3: van der Waals magnets



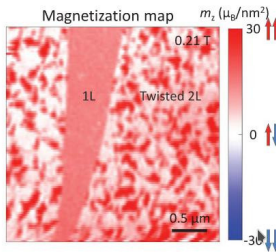
L. Thiel et al. *Science* 364 (2019), 973–976



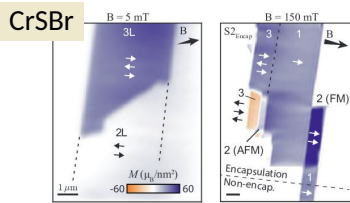
Q.-C. Sun et al. *Nat. Commun.* 12 (2021), 1989



F. Fabre et al. *Phys. Rev. Mater.* 5 (2021), 034008

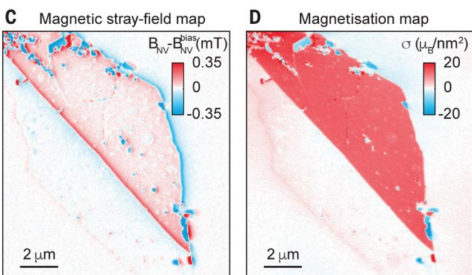
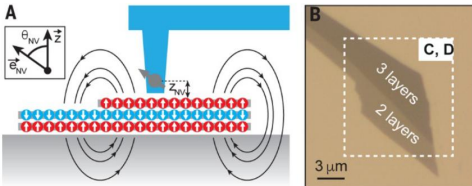


T. Song et al. *Science* 374 (2021), 1140



M. A. Tschudin et al. *arXiv* 2312.09279 (2023)

# Reverse propagation to compute M maps



- Reconstruction of ferromagnetic magnetization density maps
- Fourier space calculation
- $\vec{M}$  needs to be aligned along a single direction ( $\alpha, \beta$ )
- Mostly reliable for out-of-plane magnetized samples

$$\begin{pmatrix} \tilde{B}_x \\ \tilde{B}_y \\ \tilde{B}_z \end{pmatrix} = \frac{-\mu_0}{2 e^q z_{NV}} \begin{pmatrix} \frac{q_x^2}{q} & \frac{q_x q_y}{q} & iq_x \\ \frac{q_x q_y}{q} & \frac{q_y^2}{q} & iq_y \\ iq_x & iq_y & -q \end{pmatrix} \begin{pmatrix} \sin \alpha \cos \beta \tilde{M}(q_x, q_y) \\ \sin \alpha \sin \beta \tilde{M}(q_x, q_y) \\ \cos \alpha \tilde{M}(q_x, q_y) \end{pmatrix}$$

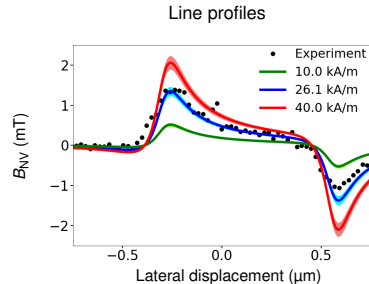
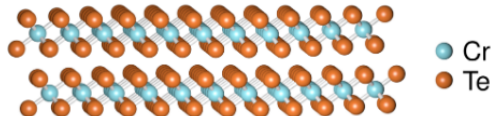
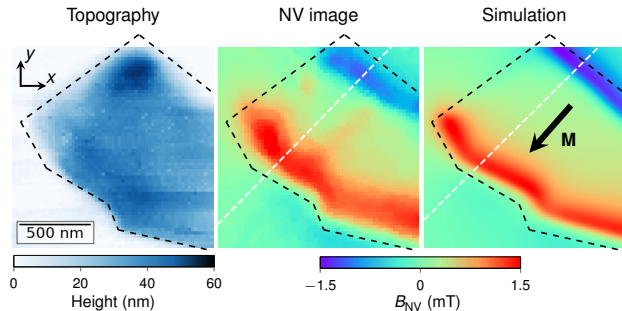
L. Thiel et al. *Science* 364 (2019), 973–976

D. Broadway et al. *Phys. Rev. Appl.* 14 (2020), 024076

# Working with a model

Collaboration: Institut Néel, Grenoble (A. Purbawati, J. Coraux, N. Rougemaille)

2D ferromagnet at room temperature  
with in-plane magnetization

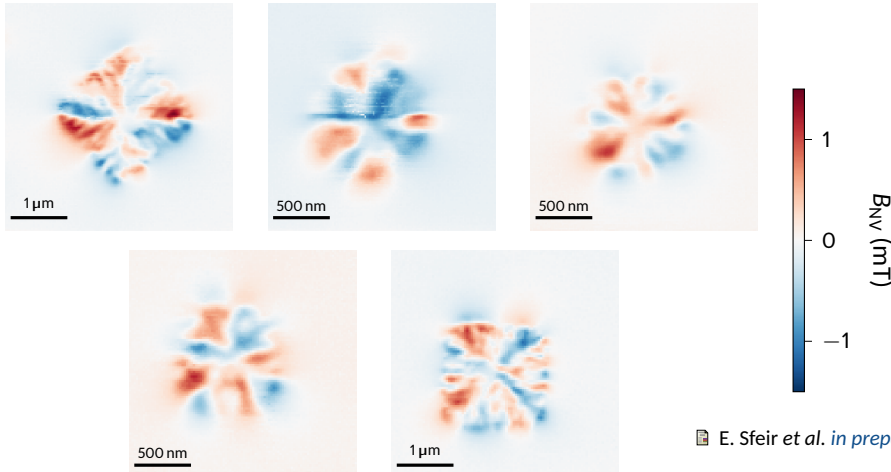


F. Fabre et al. *Phys. Rev. Mater.* 5 (2021), 034008

# Vortices!

Collaboration: Spintec, Grenoble (F. Bonnell, M. Jamet)

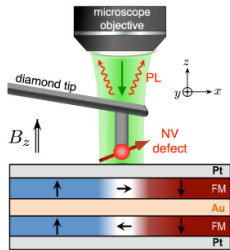
At zero field, we observe vortices in microstructured  $\text{Fe}_5\text{GeTe}_2$  (also an in-plane RT magnet):



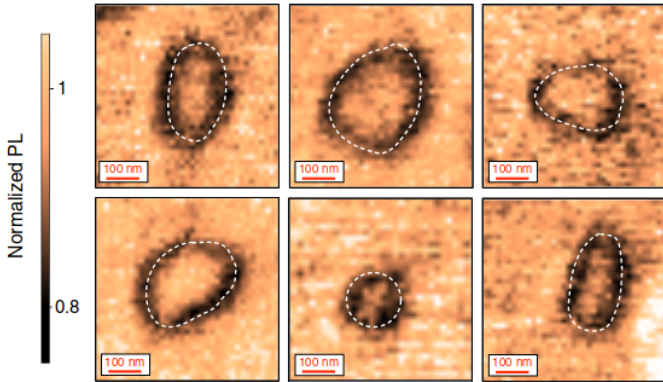
# Outline

1. The NV center in diamond as a quantum sensor
2. Dismantling the scanning NV microscope
3. Quantitative ODMR experiments
  - Principle of the measurement
  - The need for a proper calibration
  - Example 1: analyzing domain walls
  - Example 2: the spin cycloid in bismuth ferrite
  - Example 3: van der Waals magnets
4. **Taking a step back: PL quenching effects**
  - Strong off-axis magnetic fields
  - Magnetic noise!
5. Relaxometry: sensing via the relaxation time
6. Coherent control of the NV center using spin waves
7. Going further: other sensors and sensing methods

# Simpler, faster but qualitative: measure the PL



Photoluminescence maps, under  $B_z = 3 \text{ mT}$

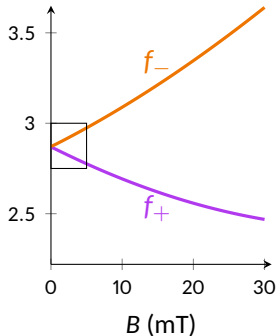


# The effect of perpendicular magnetic field

“Strong” field not oriented along the NV axis

→ Mixing of the states  $m_s = 0, \pm 1$ , which are not eigenstates anymore

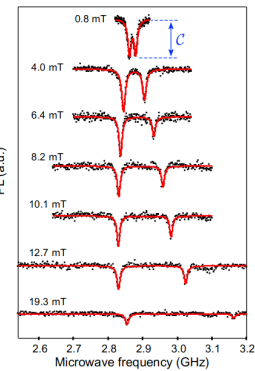
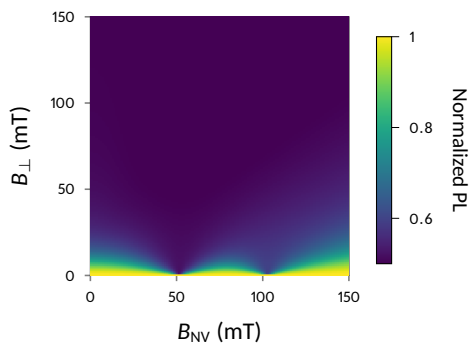
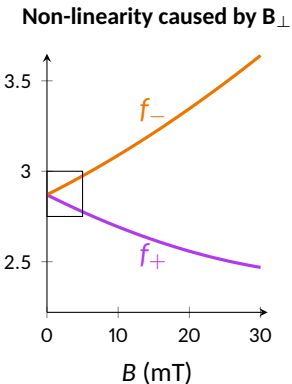
Non-linearity caused by  $B_{\perp}$



# The effect of perpendicular magnetic field

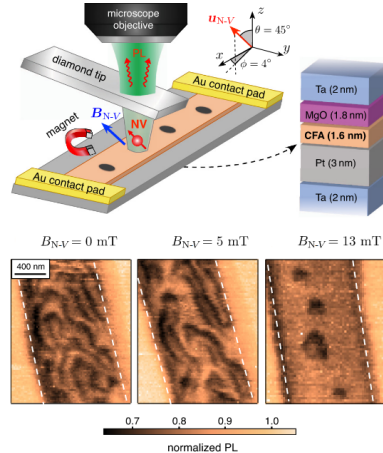
“Strong” field not oriented along the NV axis

→ Mixing of the states  $m_s = 0, \pm 1$ , which are not eigenstates anymore

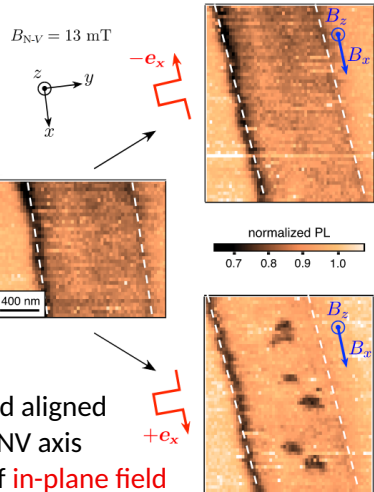
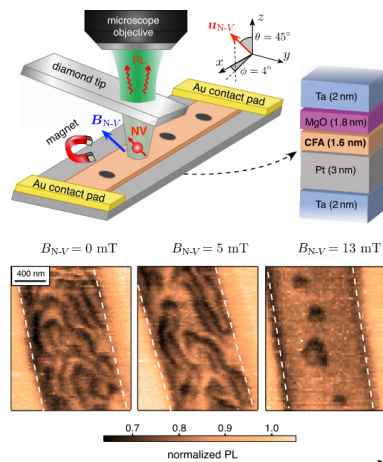


J.-P. Tetienne et al. New J. Phys. 14 (2012), 103033

# Skyrmion nucleation in PL quenching mode



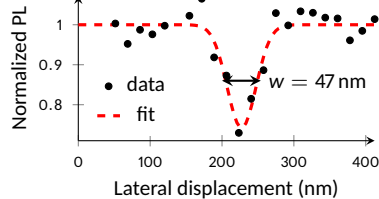
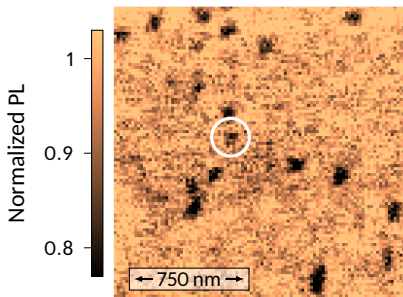
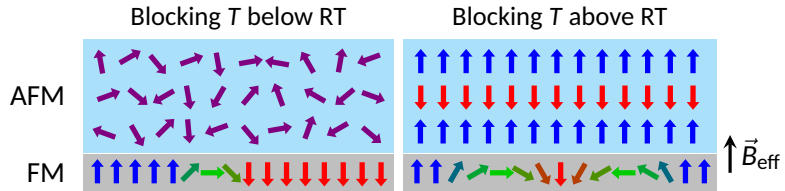
# Skyrmion nucleation in PL quenching mode



Applied field aligned  
with the NV axis

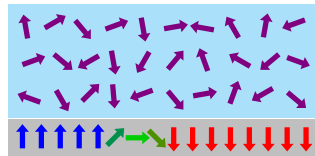
→ Observation of in-plane field  
assisted nucleation

# Skyrmions stabilized by exchange-bias

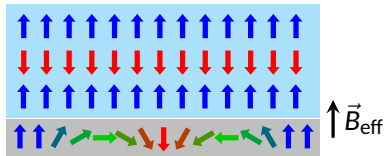


# Skyrmions stabilized by exchange-bias

Blocking  $T$  below RT

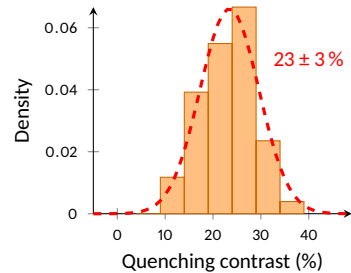


Blocking  $T$  above RT

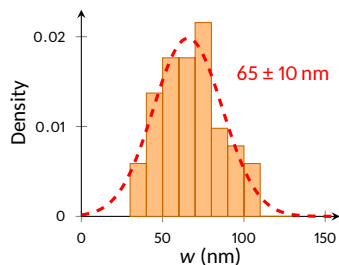
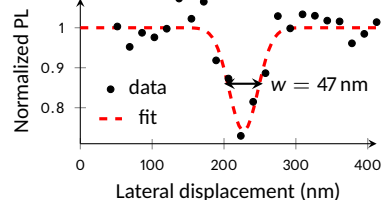
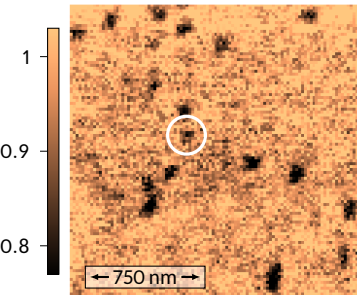


AFM

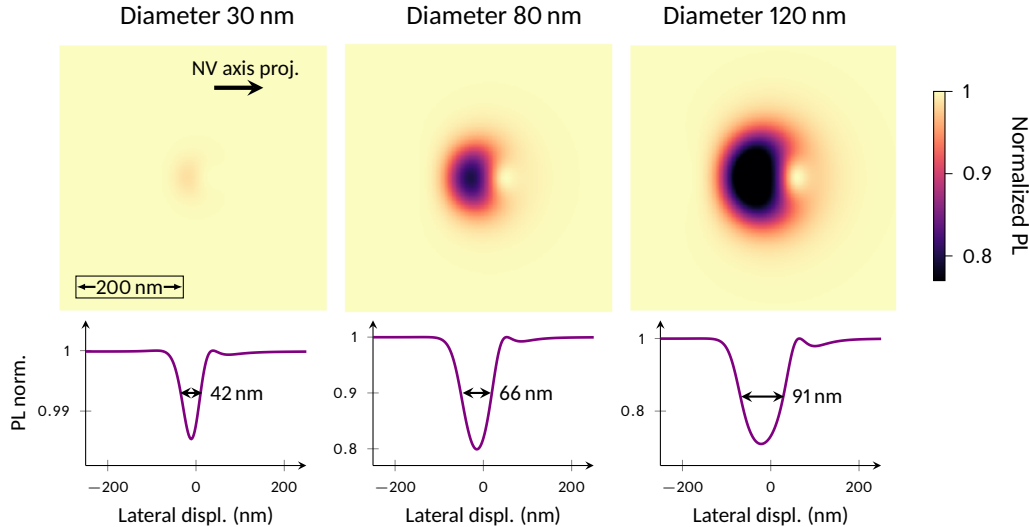
FM



Normalized PL



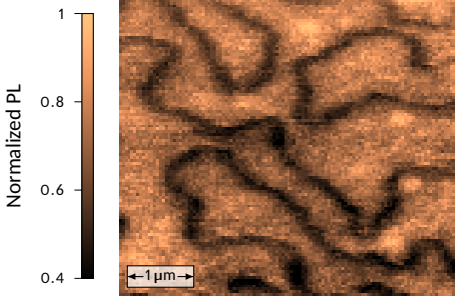
# Trying to extract quantitative information



# Noise: another source of PL quenching

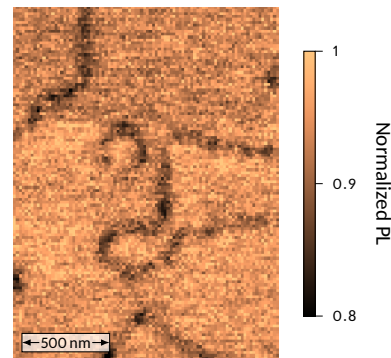
Thick ferromagnet

[Pt / Co (0.65 nm)]<sub>4</sub>



Synthetic antiferromagnet

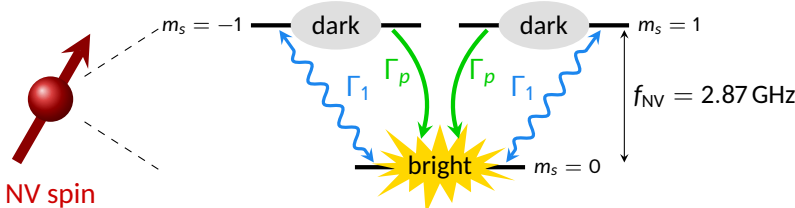
Pt / Co (0.65 nm) / Ru / Pt / Co (0.65 nm) / Ru



# Outline

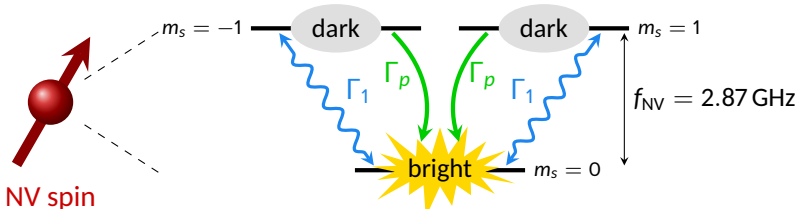
1. The NV center in diamond as a quantum sensor
2. Dismantling the scanning NV microscope
3. Quantitative ODMR experiments
  - Principle of the measurement
  - The need for a proper calibration
  - Example 1: analyzing domain walls
  - Example 2: the spin cycloid in bismuth ferrite
  - Example 3: van der Waals magnets
4. Taking a step back: PL quenching effects
  - Strong off-axis magnetic fields
  - Magnetic noise!
5. **Relaxometry: sensing via the relaxation time**
6. Coherent control of the NV center using spin waves
7. Going further: other sensors and sensing methods

# Effect of magnetic noise on the NV center

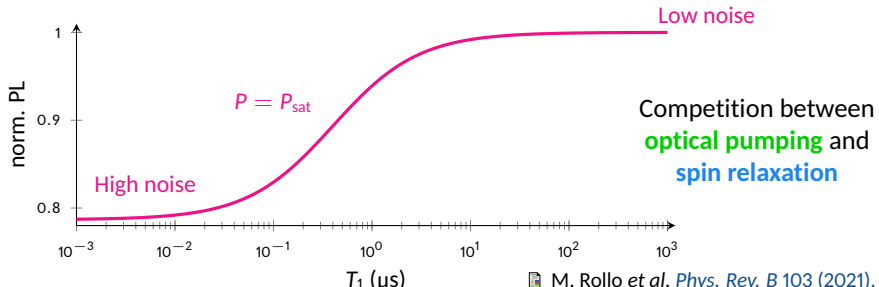


Relaxation rate  $\Gamma_1 \propto S_{B_\perp}(f_{\text{NV}})$  magnetic field spectral density at the resonance frequency  $f_{\text{NV}}$

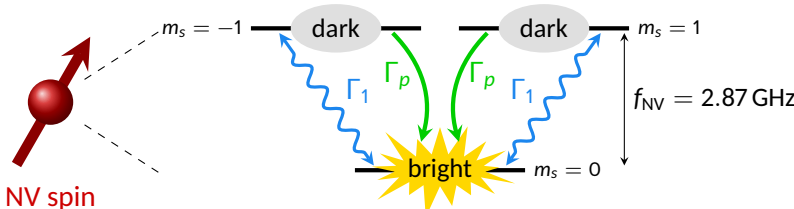
# Effect of magnetic noise on the NV center



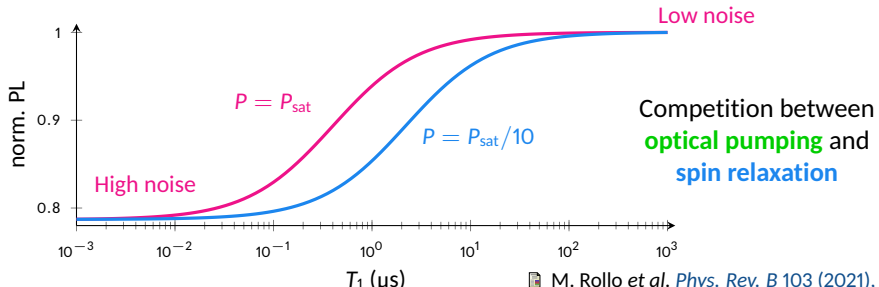
Relaxation rate  $\Gamma_1 \propto S_{B_\perp}(f_{\text{NV}})$  magnetic field spectral density at the resonance frequency  $f_{\text{NV}}$



# Effect of magnetic noise on the NV center

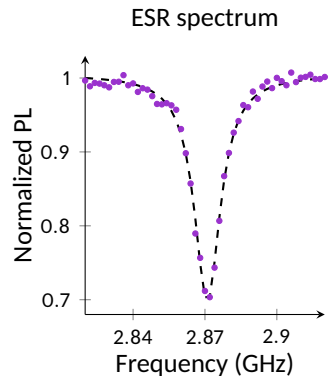
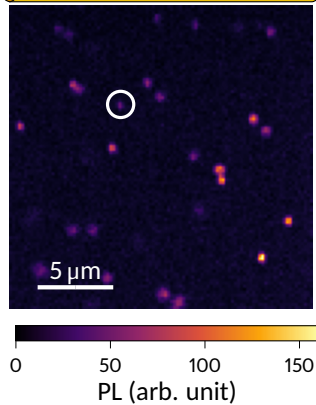
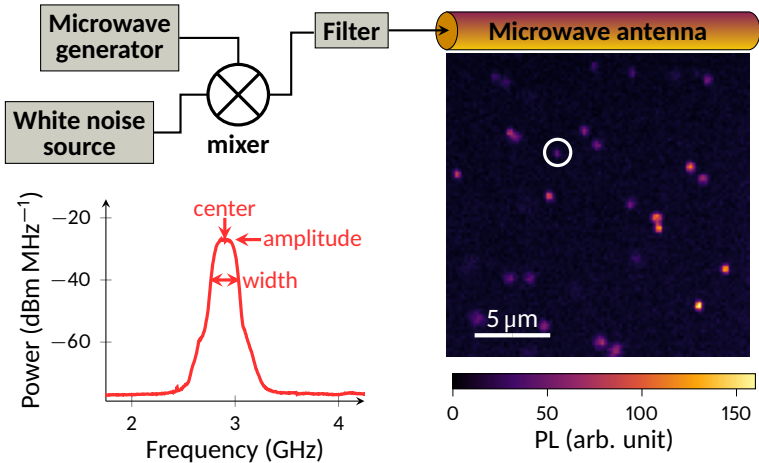


Relaxation rate  $\Gamma_1 \propto S_{B_\perp}(f_{\text{NV}})$  magnetic field spectral density at the resonance frequency  $f_{\text{NV}}$

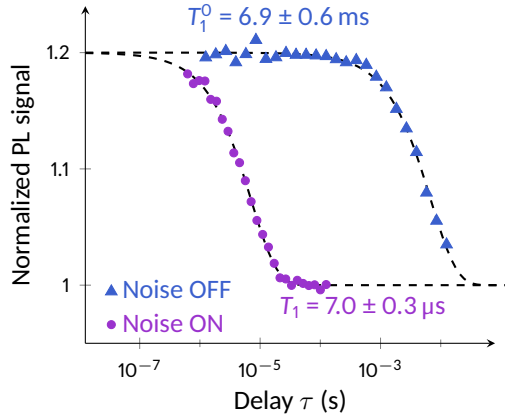
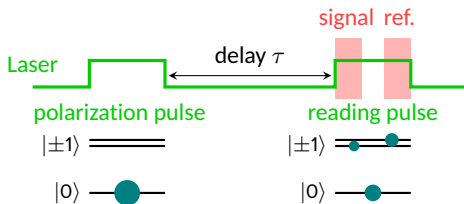
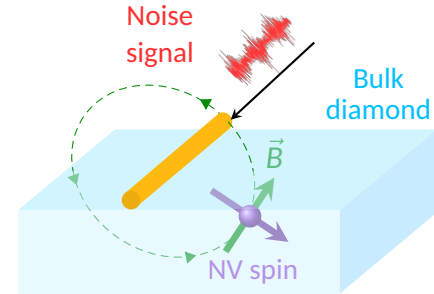


# Experimental investigation

Collaboration: C2N, Palaiseau (Thibaut Devolder)

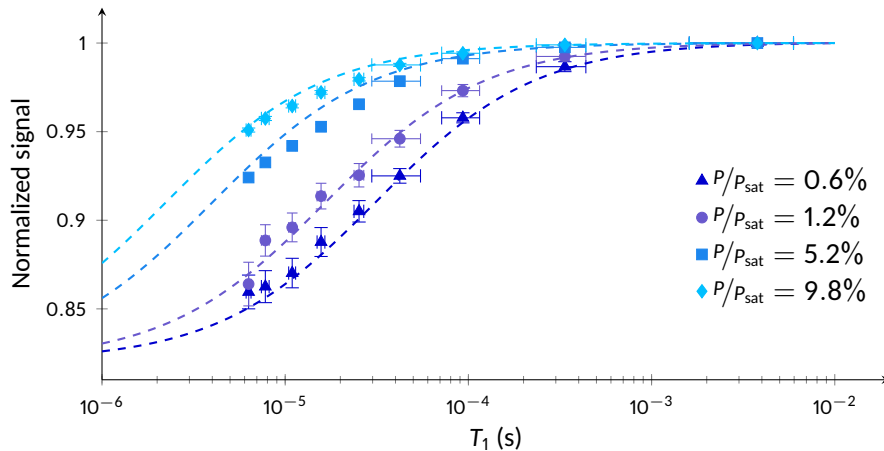


# Acceleration of the relaxation with noise



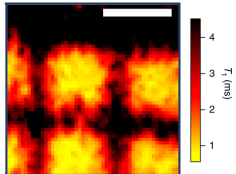
Noise spectrum centered  
at the NV transition frequency

# Evolution of the PL with noise



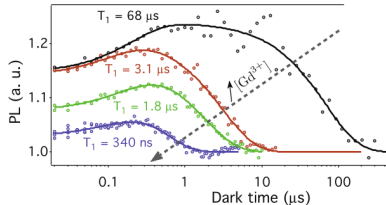
# Applications of NV relaxometry

## Measurement of Johnson noise: conductivity



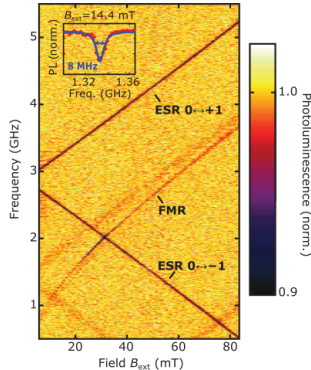
■ A. Ariyaratne et al. *Nat. Commun.* 9 (2018), 2406

## Detection of fluctuating magnetic particles



■ J.-P. Tetienne et al. *Phys. Rev. B* 87 (2013), 235436

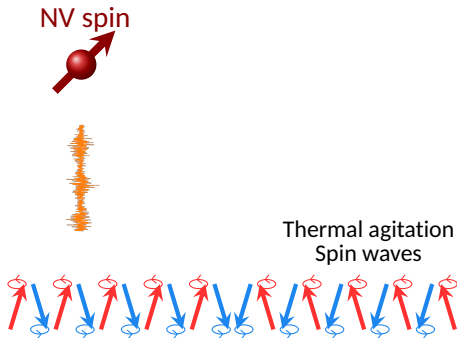
## Investigation of spin waves



■ C. Du et al. *Science* 357 (2017), 195

# Relaxometry to image antiferromagnets

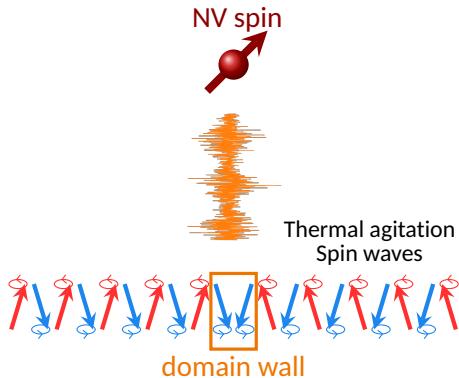
Principle: spin waves have different frequencies when they are confined inside domain walls



B. Flebus *et al.* *Phys. Rev. B* 98 (2018), 180409

# Relaxometry to image antiferromagnets

Principle: spin waves have different frequencies when they are confined inside domain walls

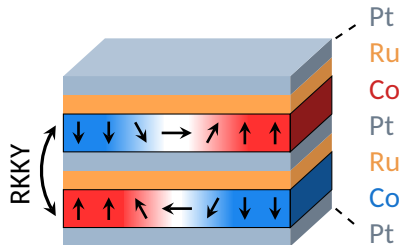


B. Flebus *et al.* *Phys. Rev. B* 98 (2018), 180409

# Synthetic antiferromagnets

Collaboration: LAF, Palaiseau (W. Legrand, K. Bouzehouane, N. Reyren, V. Cros)

Two **ferromagnetic** layers coupled **antiferromagnetically**

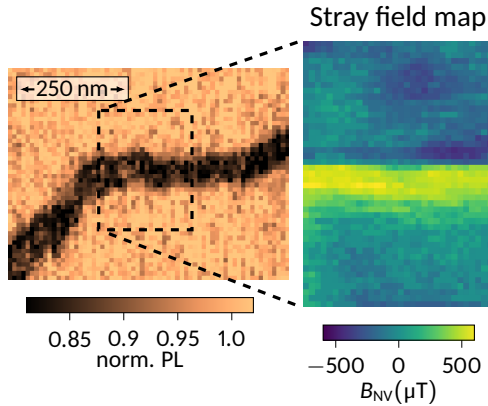
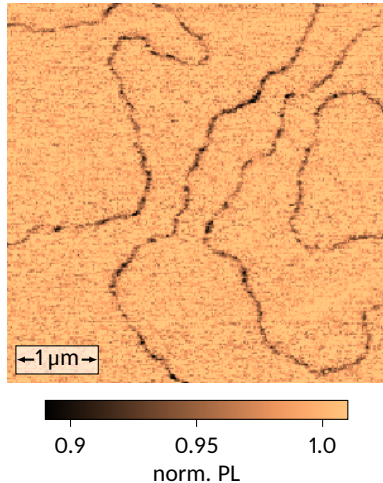


- No net magnetic moment
- Small stray field (vertical shift)
- Highly tunable properties
- Spin wave frequencies in the few GHz range

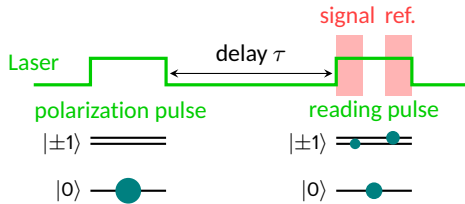
→ Perfect **test system**  
for noise imaging!

W. Legrand et al. *Nat. Mater.* 19 (2020), 34

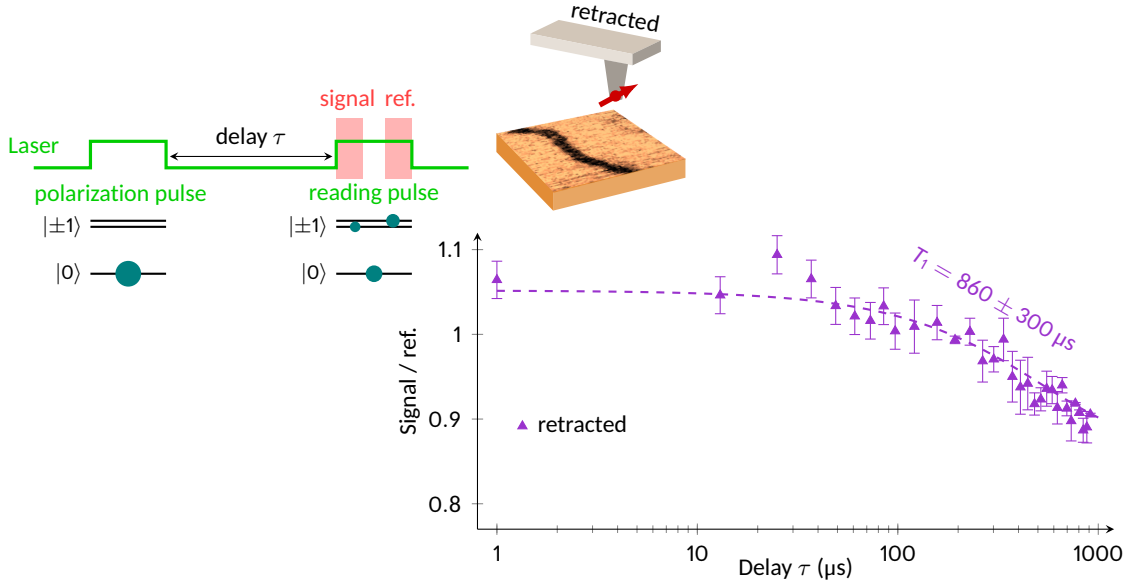
# Detection of domain walls by relaxometry



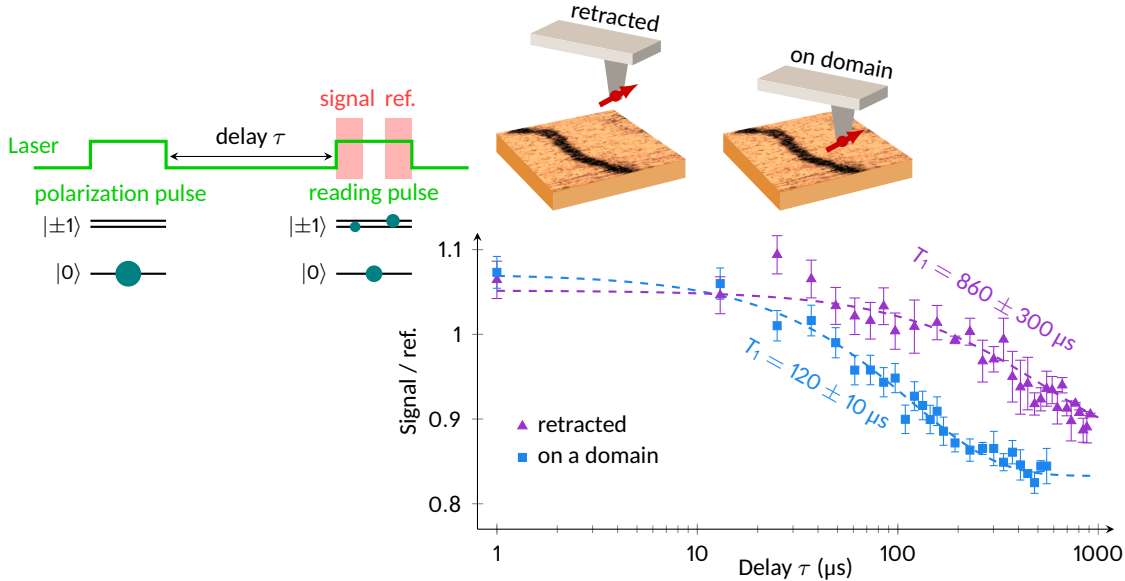
# Local variation of the relaxation time



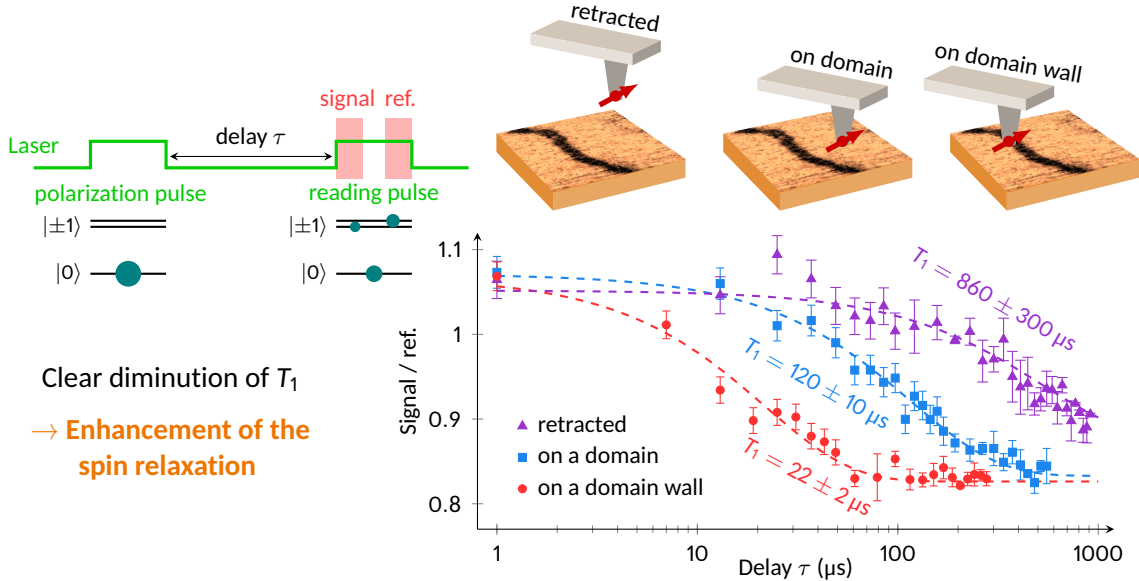
# Local variation of the relaxation time



# Local variation of the relaxation time

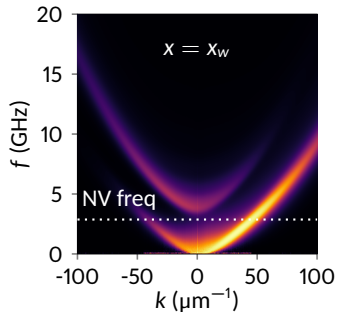
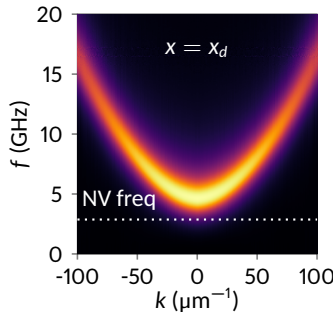
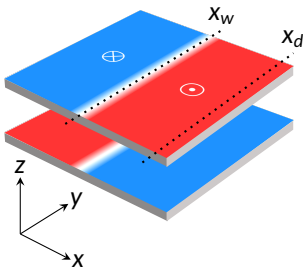


# Local variation of the relaxation time



# Origin of the noise: spin waves

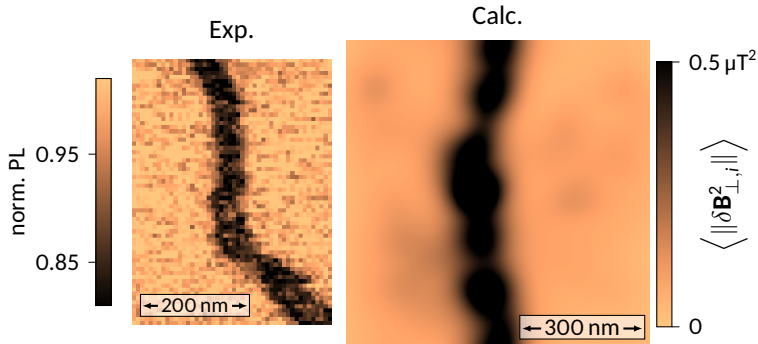
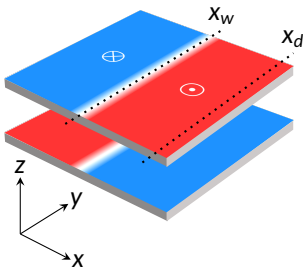
Collaboration: C2N, Palaiseau (J.-P. Adam, J.-V. Kim)



- NV frequency slightly below the gap, in the tail of power spectral density, which is the reason why we detect some noise when approaching the tip.
- No gap in the domain walls, presence of modes at the NV frequency: **the NV center is more sensitive to the noise from the walls!**

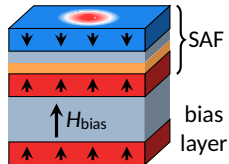
# Origin of the noise: spin waves

Collaboration: C2N, Palaiseau (J.-P. Adam, J.-V. Kim)

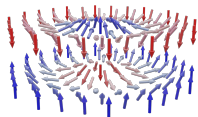


- NV frequency slightly below the gap, in the tail of power spectral density, which is the reason why we detect some noise when approaching the tip.
- No gap in the domain walls, presence of modes at the NV frequency: **the NV center is more sensitive to the noise from the walls!**

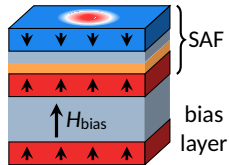
# Skyrmions stabilized by a bias layer



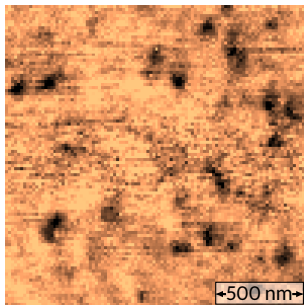
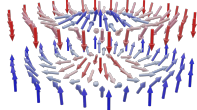
W. Legrand et al. *Nat. Mater.* 19 (2020), 34



# Skyrmions stabilized by a bias layer

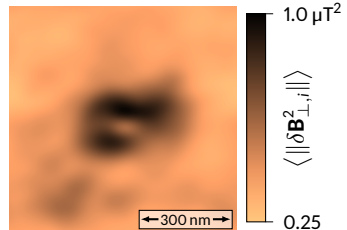
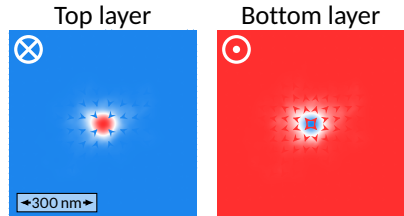


■ W. Legrand et al. *Nat. Mater.* 19 (2020), 34



0.9  
1.0

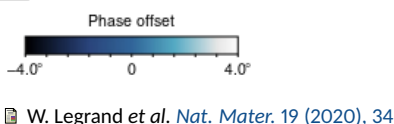
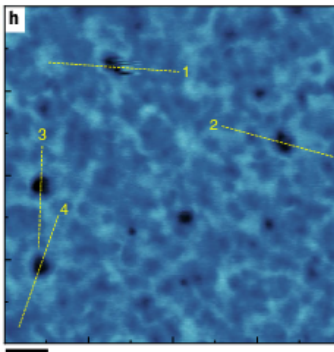
norm. PL



We are not probing the internal modes but the scattering of spin waves on the skyrmions

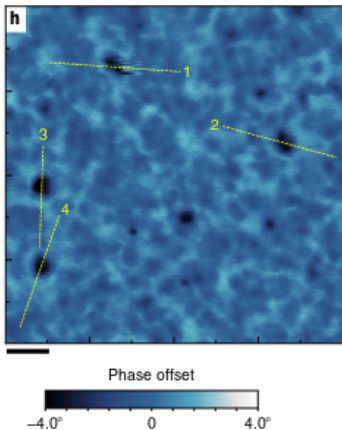
# Are these really skyrmions?

MFM under oop field 110 mT

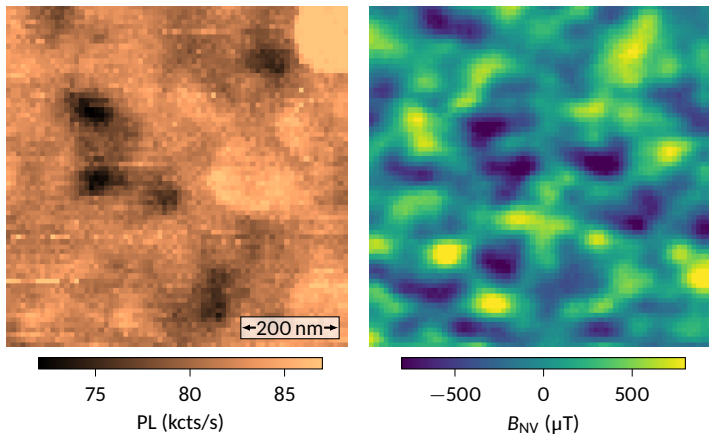


# Are these really skyrmions?

MFM under oop field 110 mT



NV images (zero field)

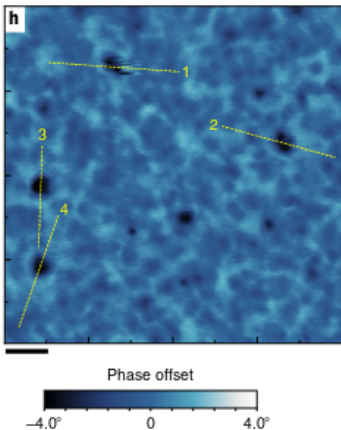


W. Legrand et al. *Nat. Mater.* 19 (2020), 34

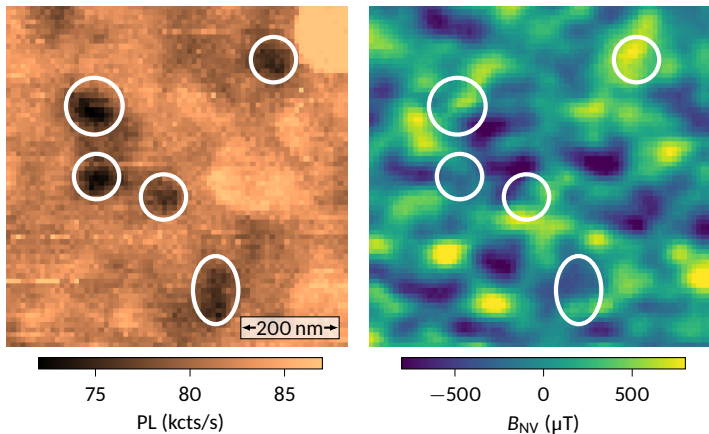
Large background fluctuations (roughness of the film)

# Are these really skyrmions?

MFM under oop field 110 mT



NV images (zero field)

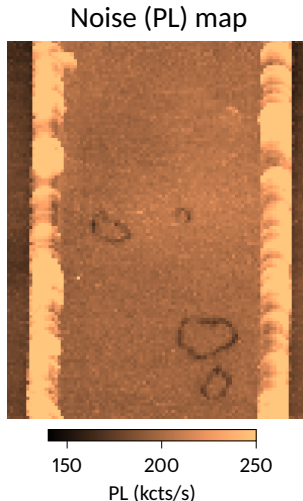
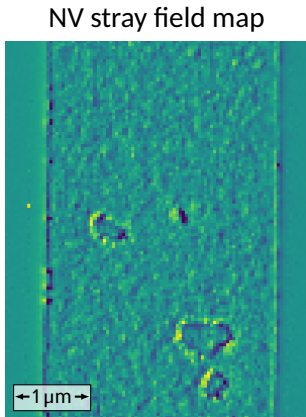


W. Legrand et al. *Nat. Mater.* 19 (2020), 34

Large background fluctuations (roughness of the film)

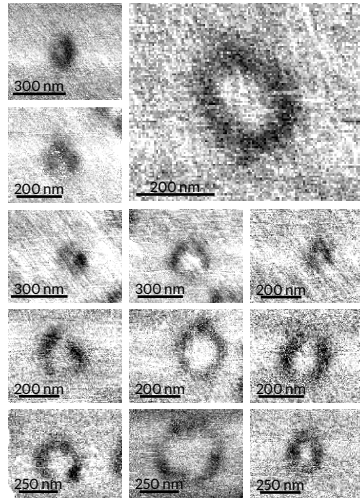
# Other samples without bias layer

Collaboration: Spintec, Grenoble (V.-T. Pham, J. Urrestarazu, O. Boulle)

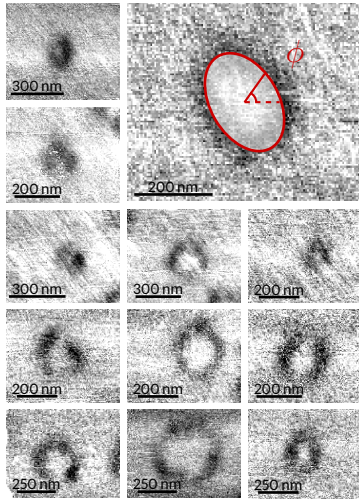


- Opp field of about 150 mT applied for nucleation
- Less background fluctuations

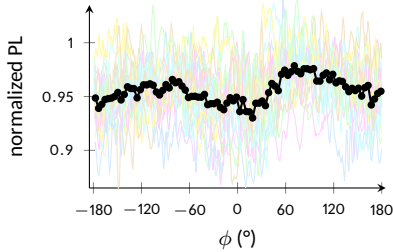
# Statistics on Néel left skyrmions



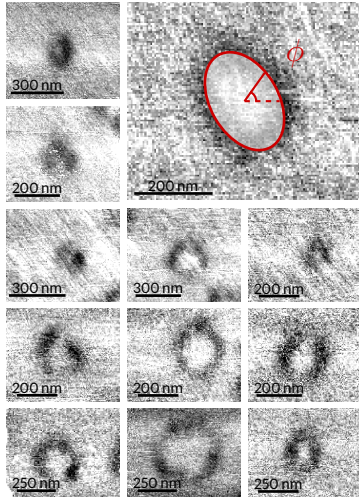
# Statistics on Néel left skyrmions



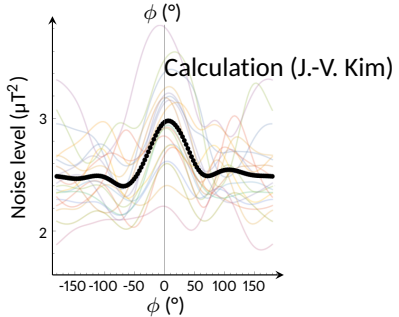
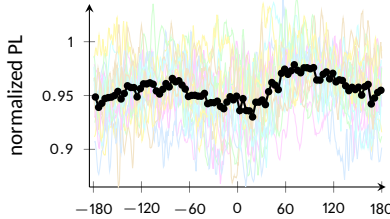
Angular variation of PL



# Statistics on Néel left skyrmions

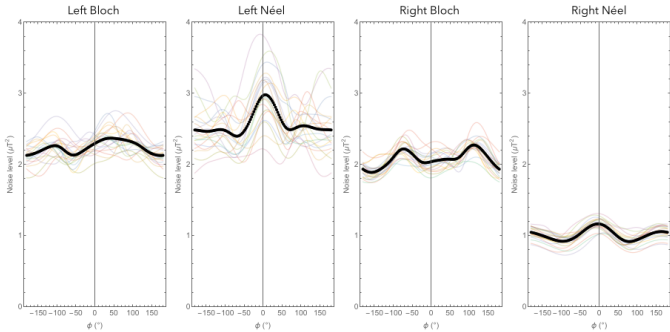


Angular variation of PL

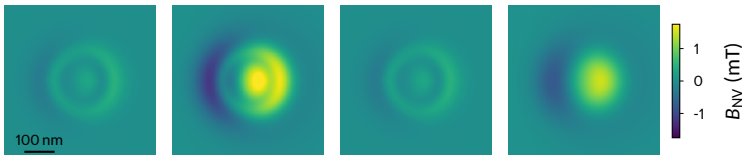


# Expected pattern on other skyrmion types

Simulated noise distribution along the contour

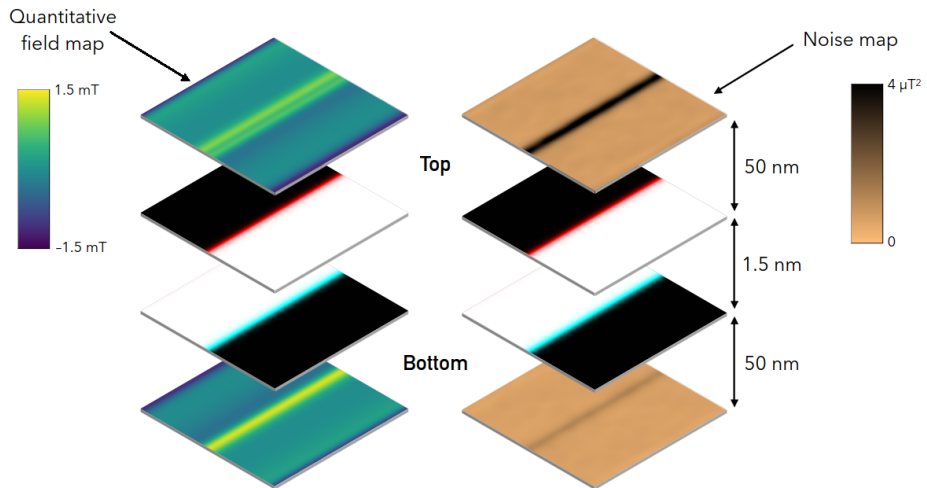


Simulated stray field maps



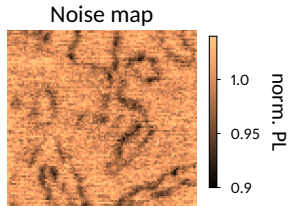
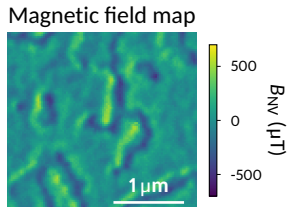
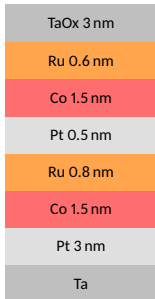
# Expected noise level for each domain wall chirality

Calculation: C2N, Palaiseau (J.-V. Kim)



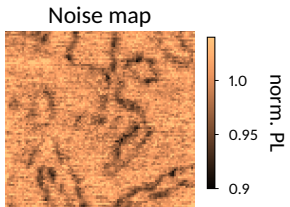
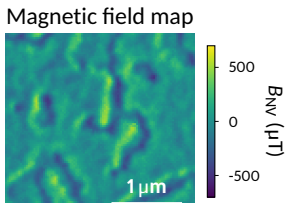
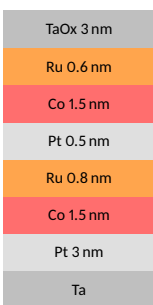
# Experiment: looking at both sides of the film

Initial stack: Néel left

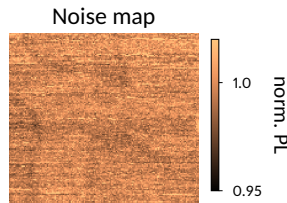
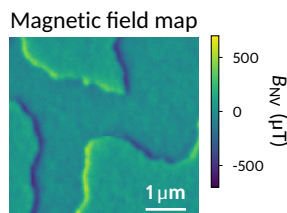


# Experiment: looking at both sides of the film

Initial stack: Néel left



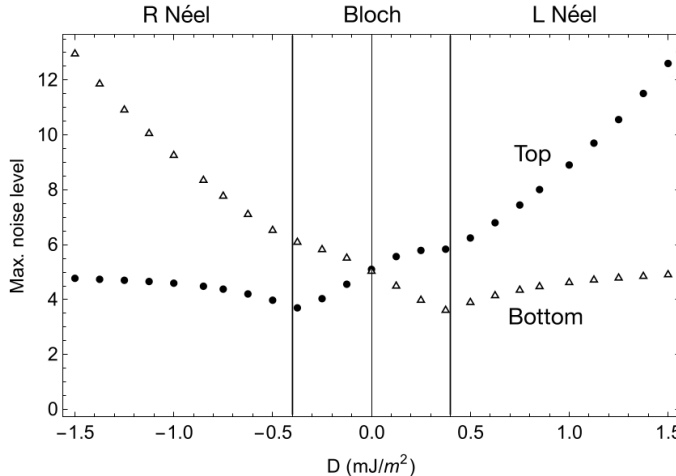
Inverted stack: Néel right



# A DMI-related effect

Calculation: C2N, Palaiseau (J.-V. Kim)

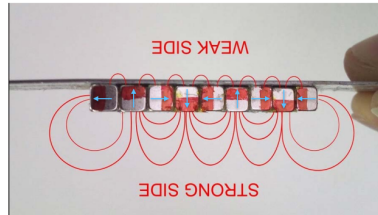
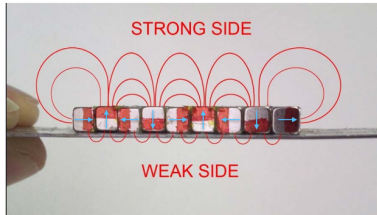
Calculation made for a **single** ferromagnetic layer



# Spin waves are like fridge magnets!

©Thibaut Devolder, C2N, Palaiseau

... and the DMI is selecting a propagation direction!



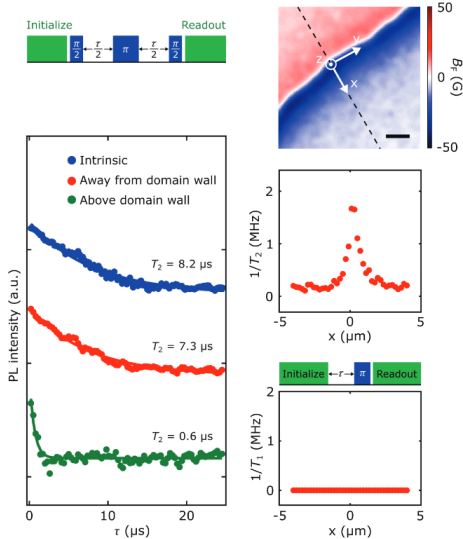
$$\begin{array}{ccccccccc} \mathbf{m}_0 & \odot & \odot & \odot & \odot & \odot & & \\ \delta\mathbf{m} & \rightarrow & \uparrow & \leftarrow & \downarrow & \rightarrow & +k & \end{array}$$

$$\begin{array}{ccccccccc} \mathbf{m}_0 & \odot & \odot & \odot & \odot & \odot & & \\ \delta\mathbf{m} & \rightarrow & \downarrow & \leftarrow & \uparrow & \rightarrow & -k & \end{array}$$

J. Mallinson. *IEEE Trans. on Mag.* 9 (1973), 678

T. Devolder. *Phys. Rev. Appl.* 20 (2023), 054057

# Decrease of $T_2$ at ferromagnetic domain walls



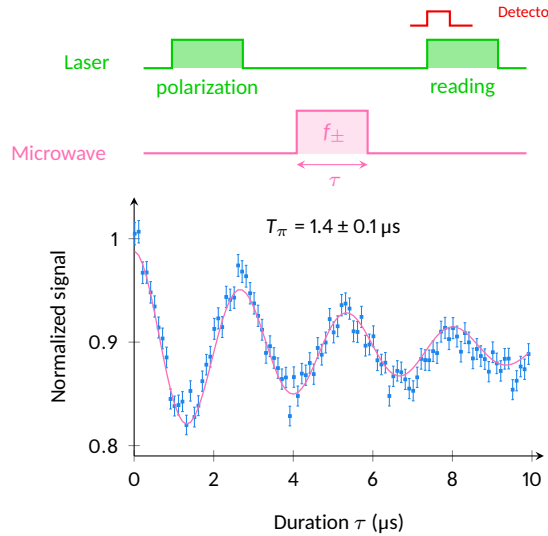
- Co/Ni/Co/Ni ferromagnetic layer
- Coherence time  $T_2$  of the NV center decreased above the domain wall
- Here  $T_1$  is not modified!
- Effect attributed to the gapless magnetic excitation of the wall

N. J. McLaughlin et al. ACS Nano 17 (2023), 25689

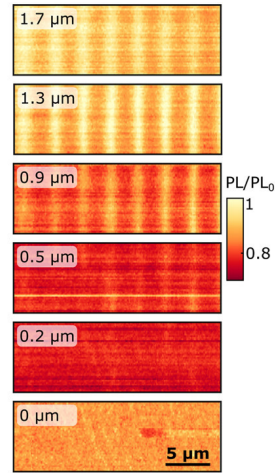
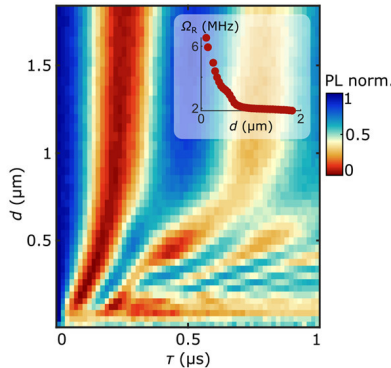
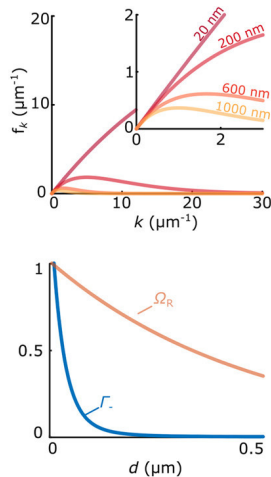
# Outline

1. The NV center in diamond as a quantum sensor
2. Dismantling the scanning NV microscope
3. Quantitative ODMR experiments
  - Principle of the measurement
  - The need for a proper calibration
  - Example 1: analyzing domain walls
  - Example 2: the spin cycloid in bismuth ferrite
  - Example 3: van der Waals magnets
4. Taking a step back: PL quenching effects
  - Strong off-axis magnetic fields
  - Magnetic noise!
5. Relaxometry: sensing via the relaxation time
6. **Coherent control of the NV center using spin waves**
7. Going further: other sensors and sensing methods

# Measurement of a Rabi oscillation

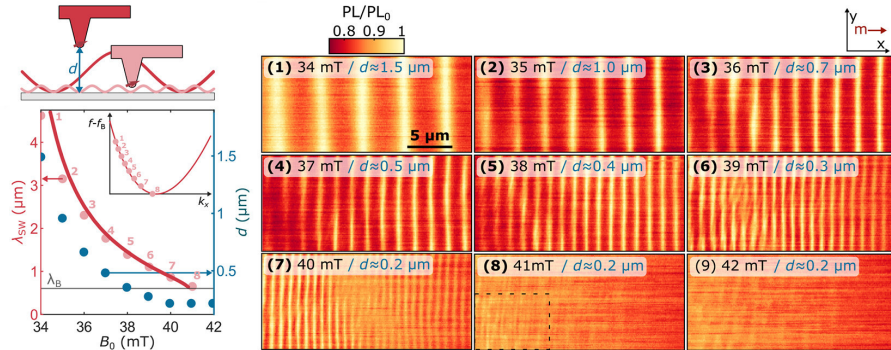


# Rabi oscillation driven by a spin wave



# Wavelength filter with $d_{\text{NV}}$

- Spin waves excited in YIG with a microwave stripline
- The wavelength of the spin wave at  $f_{\pm}$  is tuned with magnetic field
- The flying distance  $d_{\text{NV}}$  is optimized to observe it in the ODMR contrast map



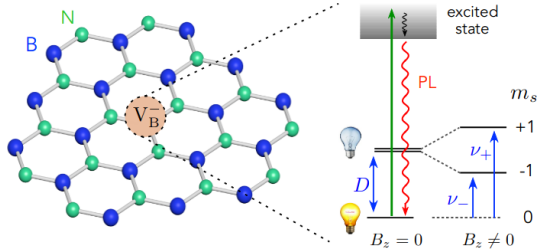
# Outline

1. The NV center in diamond as a quantum sensor
2. Dismantling the scanning NV microscope
3. Quantitative ODMR experiments
  - Principle of the measurement
  - The need for a proper calibration
  - Example 1: analyzing domain walls
  - Example 2: the spin cycloid in bismuth ferrite
  - Example 3: van der Waals magnets
4. Taking a step back: PL quenching effects
  - Strong off-axis magnetic fields
  - Magnetic noise!
5. Relaxometry: sensing via the relaxation time
6. Coherent control of the NV center using spin waves
7. Going further: other sensors and sensing methods

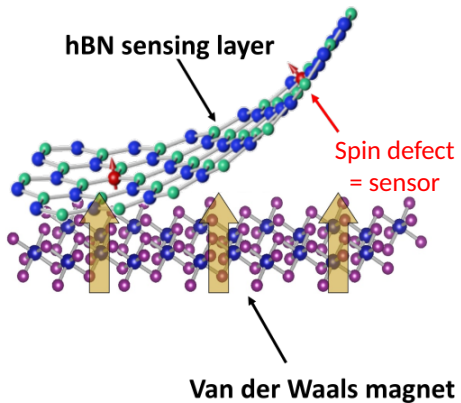
# Boron vacancies in h-BN

Optically-active spin defect in h-BN found in 2020

■ A. Gottscholl et al. *Nat. Mater.* 19 (2020), 540

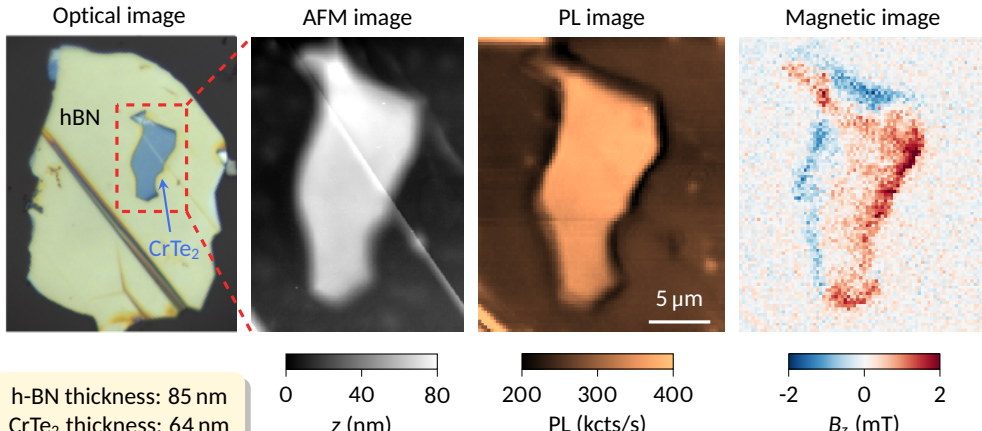


■ P. Kumar et al. *Phys. Rev. Appl.* 18 (2022), L061002



# Imaging with boron vacancies

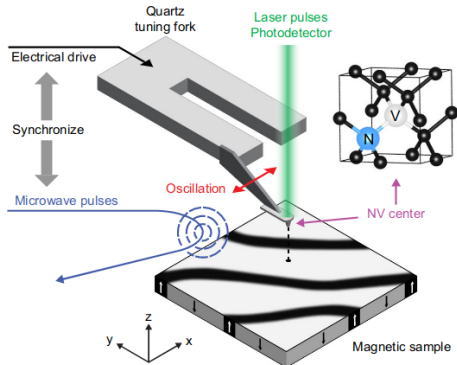
Collaboration: Institut Néel, Grenoble and LPCNO, Toulouse



- P. Kumar et al. *Phys. Rev. Appl.* 18 (2022), L061002
- M. Huang et al. *Nat. Commun.* 13 (2022), 5369
- A. J. Healey et al. *Nat. Phys.* 19 (2023), 87

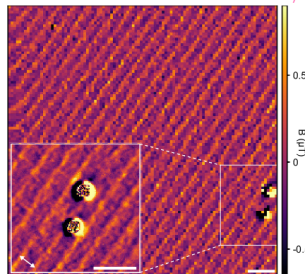
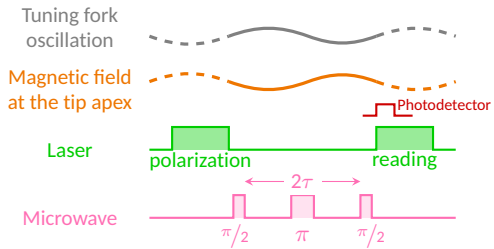
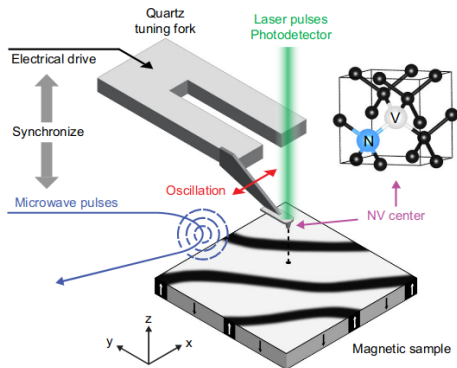
# Advanced mode: gradiometry

Use a spin echo sequence to improve the magnetic sensitivity



# Advanced mode: gradiometry

Use a spin echo sequence to improve the magnetic sensitivity

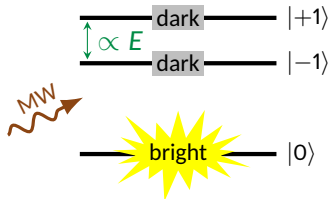


Stray field from  
atomic steps visible  
in the A-type  
antiferromagnet  
 $\text{Cr}_2\text{O}_3$

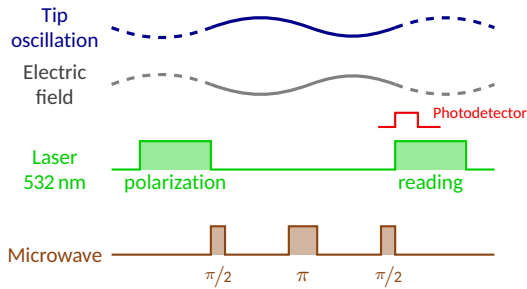
# Electric field sensing

To investigate ferroelectrics!

## Stark shift



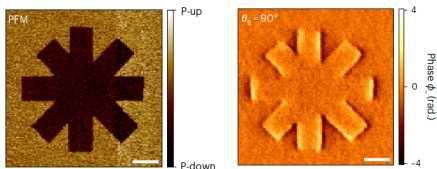
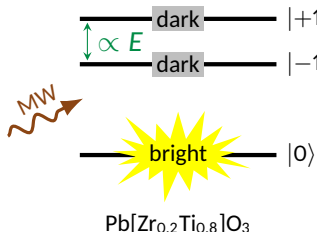
- Need to apply off-axis field to avoid that Zeeman effect dominates
- Electric susceptibilities rather small  
→ spin echo sequences



# Electric field sensing

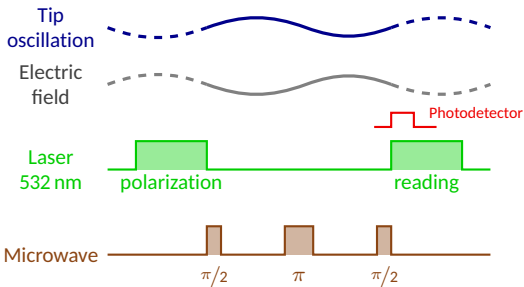
To investigate ferroelectrics!

## Stark shift



W. S. Huxter et al. *Nat. Phys.* 19 (2023), 644

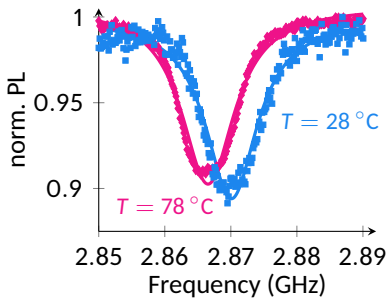
- Need to apply off-axis field to avoid that Zeeman effect dominates
- Electric susceptibilities rather small  
→ spin echo sequences



Z. Qiu et al. *npj Quantum Info.* 8 (2022), 107

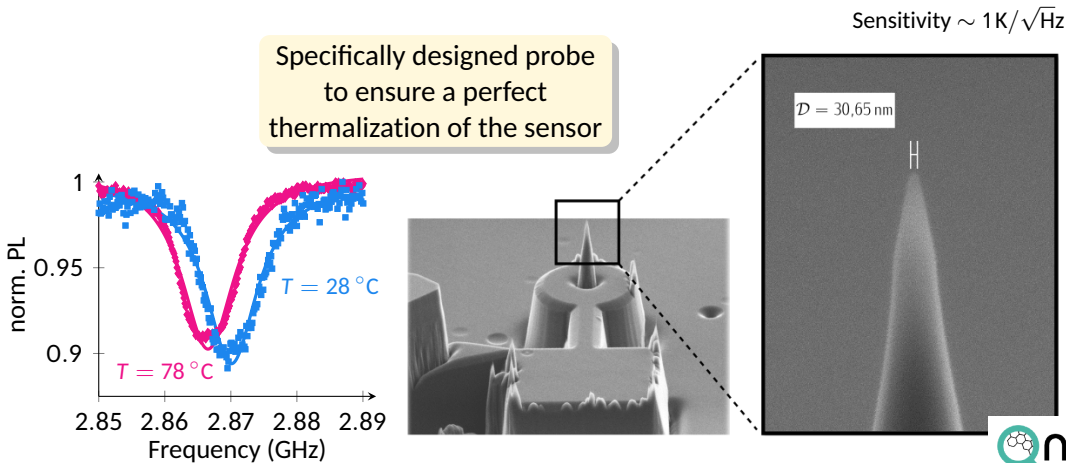
# Temperature sensing

Crystal dilatation → Shift of the zero-field splitting

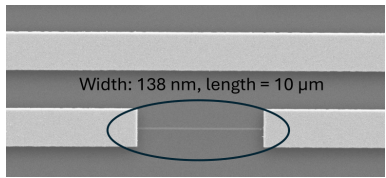


# Temperature sensing

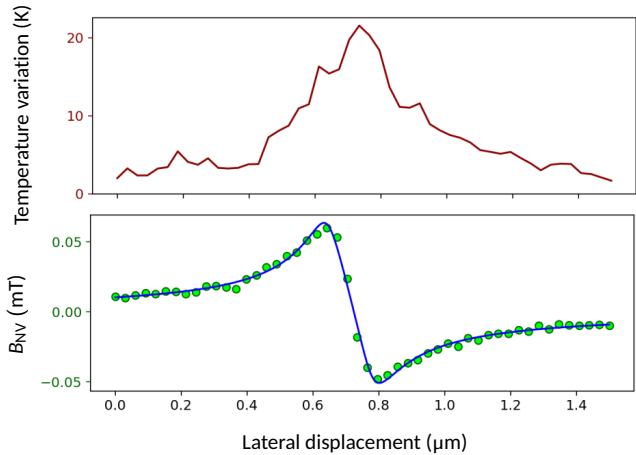
Crystal dilatation → Shift of the zero-field splitting



# First results on thermometry



Nanowire of doped Si from CEA Grenoble  
 $I = 60 \mu\text{A}$



# A versatile microscope to probe condensed matter

Magnetic field

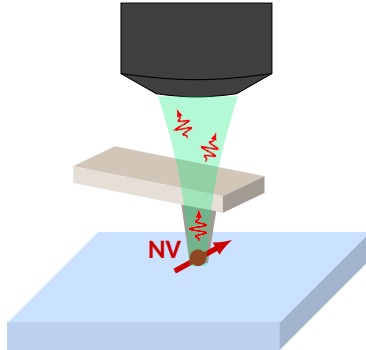
(Anti)ferromagnetic  
textures

Currents

Magnetic noise

Spin waves

Conductivity



Electric field

Ferroelectric  
textures

Temperature

Localized  
hot spots

Interested in NV microscopy?  
Join us!



<https://solidstatequantumtech-12c.fr/>